Published in final edited form as:
Mater Sci Eng C Mater Biol Appl. 2014 July 1; 40: 180–188. doi:10.1016/j.msec.2014.03.065.

Biodegradable electrospun nanofibers coated with platelet-rich plasma for cell adhesion and proliferation

Luis Díaz-Gómez[1,2], **Carmen Alvarez-Lorenzo**[1,*], **Angel Concheiro**[1], **Maite Silva**[2], **Fernando Dominguez**[3], **Faheem A. Sheikh**[4], **Travis Cantu**[4], **Raj Desai**[4], **Vanessa L. Garcia**[4], and **Javier Macossay**[4,*]

[1]Departamento de Farmacia y Tecnología Farmacéutica, Facultad de Farmacia, Universidad de Santiago de Compostela, 15872-Santiago de Compostela, Spain

[2]Instituto de Ortopedia y Banco de Tejidos Musculoesqueléticos, Universidad de Santiago de Compostela, 15872-Santiago de Compostela, Spain

[3]Fundación Publica Galega de Medicina Xenómica, Santiago de Compostela, Spain

[4]Department of Chemistry, University of Texas Pan American, Edinburg, TX 78541, USA

Abstract

Biodegradable electrospun poly(ε-caprolactone) (PCL) scaffolds were coated with platelet-rich plasma (PRP) to improve cell adhesion and proliferation. PRP was obtained from human buffy coat, and tested on human adipose-derived mesenchymal stem cells (MSC) to confirm cell proliferation and cytocompatibility. Then, PRP was adsorbed on the PCL scaffolds via lyophilization, which resulted in uniform sponge-like coating of 2.85 (s.d. 0.14) mg/mg. The scaffolds were evaluated regarding mechanical properties (Young's modulus, tensile stress and tensile strain), sustained release of total protein and growth factors (PDGF-BB, TGF-β1 and VEGF), and hemocompatibility. MSC seeded on the PRP-PCL nanofibers showed an increased adhesion and proliferation compared to pristine PCL fibers. Moreover, the adsorbed PRP enabled angiogenesis features observed as neovascularization in a chicken chorioallantoic membrane (CAM) model. Overall, these results suggest that PRP-PCL scaffolds hold promise for tissue regeneration applications.

*Corresponding authors: carmen.alvarez.lorenzo@usc.es, Tel: +34 981563100, Fax: +34 981547148; jmacossay@utpa.edu; Tel.: (956) 665-3377; fax: (956) 665-5006.

Supplementary material: Alcian blue and ALP staining images of MSC cultured in control and 10% PRP medium for 7 days; SEM microphotographs of electrospun PCL solely scaffolds at 2000× and 8000×; PCL scaffold degradation profile in PBS; Images of the water contact angle measurement in PCL and PRP-PRP scaffolds; Fluorescent Hoescht staining of MSC nuclei on PCL (A) and PRP-PCL (B) scaffolds after 36 h (A1, B1) and 6 days (A2, B2) of culture.

Keywords

electrospinning; PCL scaffold; platelet-rich plasma; cell proliferation; angiogenesis; growth factors sustained release

1. Introduction

Electrospinning was first described in patents by Cooley in the early 1900's [1] and the first reports on using this technique to obtain cellulose acetate, cellulose propionate and wool-cellulose acetate fibers were published in the 1930's [2]. The technique consists of placing a polymer solution in a syringe and connecting it to a high power supply, which generates a high voltage difference (5 kV to 30 kV) between the syringe needle and a grounded target. As the polymer is ejected, the electrical charges on the polymer solution promote solvent evaporation, thus forming a dry polymer fiber that travels in a chaotic pattern and deposits on the grounded target [3]. Variables of the process, such as polymer concentration, solvent volatility, solution conductivity, applied voltage, solution flow rate, and gap between syringe and collector greatly determine fiber properties [4].

Nanofibrous scaffolds obtained through electrospinning process consist of fibers with an average diameter between 50 and 5000 nm and tunable surface area, morphology, mechanical performance or length/diameter ratio [5]. A large variety of natural and synthetic materials can be electrospun to prepare suitable scaffolds for cell seeding and proliferation, being this technique particularly convenient for regenerative medicine [6]. For example, electrospinning can render aligned nanofibers with spatial distribution similar to organized tissues, suitable for tendon regeneration [7], or aligned-to-random scaffolds for mimicking the structure of the tendon-to-bone insertion site [8]. Layered composite electrospun scaffolds have been shown useful to regenerate endothelium due to their analogous structure with natural blood vessels [9], and nanofibrous electrospun scaffolds may be suitable as dermal substitutes for skin regeneration [10]. Moreover, the technique enables the combination of natural biomaterials, synthetic polymers and growth factors [11].

Poly(ε-caprolactone) (PCL) is a biocompatible and biodegradable polymer suitable for preparing electrospun nanofibers. Unlike other polymers extensively used in biomedical applications, such as polylactic acid (PLA) or polyglycolic acid (PGA), hydrolysis of PCL does not produce a local acidic environment that could compromise cell growth [12–14]. Nevertheless, mammalian cell attachment on PCL scaffolds is limited due to its hydrophobicity and inertness. This drawback can be overcome by means of hydrophilization techniques, such as wet chemical and plasma treatment, surface graft polymerization or physical adsorption [15, 16], which also enable the incorporation of bioactive molecules to the scaffold. For example, drugs, proteins and gene material have been adsorbed onto scaffold surfaces to form coatings that promote cell adhesion and proliferation [15, 17, 18].

Platelet-rich plasma (PRP) is becoming an attractive alternative to the use of expensive and immunological-risky recombinant growth factors, due to its autologous nature and easiness of obtainment [19]. Platelets play a crucial role in the inflammatory response and the regeneration process; they release high amounts of biologically active growth factors, some

of which are involved in different healing stages. PRP growth factors include transforming growth factor (TGF-β1), basic fibroblast growth factor (bFGF), epidermal growth factor (EGF), vascular endothelial growth factor (VEGF), insulin-like growth factor, and platelet derived growth factor (PDGF) [20] with chemotactic, mitogenic, morphogenic and metabolic effects, which are involved in cell recruitment, proliferation, morphogenesis and differentiation. Growth factors also play a remarkable role in the cell-extracellular matrix communication during regeneration activity [21]. Electrospinning of PRP solely or combined with biodegradable polymers, such as PCL or PGA, has been also evaluated [22]. The resultant scaffolds showed excellent penetration and proliferation of adipose-derived stem cells. PRP has been loaded in chitosan gels and sponges for sustained release of growth factors [23]. Just recently, PRP has been physically adsorbed onto Vicryl® (PGA fibers) and then freeze-dried as a way to preserve the related growth factors until use, instead of the immediate preparation of the PRP from patients' blood [24].

The aim of this study was to prepare bioactive PCL scaffolds by coating electrospun fibers with PRP via impregnation followed by freeze-drying. It was hypothesized that the adsorption of PRP on the fibers would enhance cell attachment and proliferation, without detrimental effects on the preparation and the mechanical behavior of the fibers. Moreover, sustained release, ideally sequential delivery, of some growth factors from the scaffold may be beneficial for tissue regeneration. Compared to direct electrospinning of polymer and PRP mixtures, coating of preformed fibers may be advantageous as it enables the fibers to be prepared according to preset protocols and then to be functionalized with PRP (from donor pools or from an specific patient) just before use. This approach can avoid concerns regarding storage and stability of the preformed fibers and also of PRP (as co-electrospinning requires dissolution of the growth factors in organic solvents) and may also enable tuning the quantity of PRP deposited according to a given application. Once implanted, PRP adsorbed on the scaffold may create an environment rich in growth factors able to promote tissue repair/regeneration.

2. Materials and methods

2.1 Materials

Poly-ε-caprolactone (PCL; M_n = 70–90K), tetrahydrofuran 99% (THF) and N,N-dimethylformamide 99.8% (DMF) were purchased from Sigma-Aldrich (St. Louis, MO, USA) and used without further purification. Mesenchymal stem cells (MSC) StemPRO® human adipose-derived stem cells were from Gibco (Invitrogen, USA), and murine fibroblasts (CCL-163) from the American Type Culture Collection (ATCC, USA). All other reagents were analytical grade.

2.2 Platelet Rich Plasma (PRP) preparation and characterization

2.2.1 PRP preparation—Human PRP was obtained from human buffy coat (Centro de Transfusión de Galicia, Spain) and transferred to 50 mL Falcon tubes (BD Bioscience, USA). The buffy coat was centrifuged at 400*g* for 15 minutes, and the supernatant rich in platelets was collected and analyzed using a Coulter counter (Beckman, USA; 100μm slit) resulting in $3{\cdot}10^6$ platelets/μL. Tubes with 1 mL of PRP were activated in separate by

freeze-thaw cycles: aliquots were stored at −80 °C for 24 hours, followed by 1 hour at room temperature and frozen again. After 3 cycles, tubes were centrifuged at 12000*g* for 10 minutes at 4 °C, and the supernatant containing growth factors was recovered and kept frozen at −80 °C until use (as liquid) or freeze-drying. Each mL of PRP led to 72.5 mg after freeze-drying. Total protein and VEGF present in freeze-dried PRP were quantified, in sextuplicate, by means of BCA analysis and an ELISA kit (RayBiotech, USA), respectively.

2.2.2 Effect of PRP on MSC proliferation—Human MSC ($2{\cdot}10^4$ cells) were seeded in 24-well plates with either 1 mL of MSC medium (MesenPro RS, 2% growth supplement MesenPro RS, Gibco USA, 1% Pen-Strep) (control) or 1 mL of PRP-rich medium (MesenPro RS:PRP solution:Pen-Strep 89:10:1 vol%; equivalent to 7.25 mg freeze-dried PRP/mL), and then incubated in a humidified atmosphere with 5% CO_2 at 37 °C. Cell proliferation was tested at 1, 3 and 7 days using the MTT assay (Roche, Switzerland) and results were read at 550 nm (UV Bio-Rad Model 680 microplate reader, USA). All experiments were carried out in triplicate.

2.2.3 Histochemical analysis of PRP effect—An Alcian blue staining was done to evaluate extracellular matrix (ECM) synthesis during MSC proliferation. MSC were seeded in 24-well plates following the same protocol as for the proliferation assay (negative control and 10% PRP supplemented medium), with the medium being renewed every 3 days. After 7 days, cells were rinsed with PBS and fixed with 4% formaldehyde solution for 30 minutes. Then, they were rinsed again with PBS and 1% Alcian blue solution in 0.1N HCl was added. After 30 minutes, wells were rinsed with 0.1N HCl and then with water. Cells were observed using light microscopy to search for blue staining indicative of synthesis of glycosaminoglycans. Differentiation of MSC to other cell lineages such as osteoblasts was evaluated recording alkaline phosphatase (ALP) activity after 7 days of growth. Cells were fixed with 4% paraformaldehyde solution for 5 minutes, washed twice with PBS and incubated in darkness with naphthol ASMX-phosphate and 0.1% fast violet in 56 mM AMPD (2-amino-2-methyl propanediol) for 30 minutes. Then, the cells were observed under light microscopy.

2.3 PCL scaffolds preparation and characterization

2.3.1 Preparation—Aliquots (4 mL) of PCL solution (10 wt.%) in a THF:DMF (1:1) were electrospun onto an aluminum grounded target placed at 24 cm from the needle tip. PCL polymer nanofibers were obtained using a 10 mL glass syringe with a 22-needle gauge (0.7 mm OD × 0.4 mm ID) at a flow rate of 0.05 mL/minutes. The flow rate was controlled using a KDS 210 pump (KD Scientific Holliston Inc., MA). The high power supply used was an ES30P-5W purchased from Gamma High Voltage Research (Ormond Beach, FL), and the equipment was attached to the needle tip through an alligator clip with a voltage difference of 25 kV.

Scaffolds (cut as disks of 1.33 cm^2 and ca. 5 mg weight) were washed with ethanol for 10 minutes and with PBS (3 times), and then each disc was immersed in activated PRP (1 mL), kept under stirring for 4 hours at 4°C, transferred to 24-well plates, and freeze-dried at

−80°C. The amount of PRP deposited on the disks was estimated gravimetrically from at least six replicate samples. Thereinafter, PRP-coated PCL is referred as PRP-PCL scaffold.

2.3.2 Physical characterization—Scanning electron microscopy (SEM) images of scaffold disks of 1.33 cm^2 were taken using a Zeiss Ultra Plus (Germany) at various magnifications after coating with a gold-palladium layer. The diameters of the nanofibers as well as the length of the pores among the fibers were measured in at least 100 different points. The mechanical behavior of the nanofiber mats (cut in the form of a “dog-bone” shape using a die that afforded samples with 2.75 mm wide at their narrowest point and a gauge length of 7.5 mm) was investigated using an INSTRON® tensile tester 5943 with a 25 N maximum load cell under a crosshead speed of 10 mm/minutes. Ten specimens were tested for tensile behavior and the average values reported. Water contact angles (10 μL) were measured at various times using a Phoenix-300 plus video-based optical contact angle measuring device fitted with SurfaceWare software (SEO, Korea). Attenuated total reflectance Fourier transform infrared (ATR-FTIR) spectra were recorded on a Varian 670-IR (Varian Inc, USA) in a 400–4000 cm^{-1} range at a resolution of 2 cm^{-1}.

2.3.3 Hydrolytic degradation—Fiber mats were immersed in USP phosphate buffer pH 7.4 at 37°C, and their erosion rate was determined monitoring the weight loss. After 5 days in buffer, mats were washed with water, dried at 37°C for 3 days, and weighed. The washing, drying, and immersion cycles were repeated 5 times until 40 days.

2.3.4 Growth factors release from PRP-PCL scaffolds—Total protein and PDGF-BB, TGF-β1 and VEGF release tests were carried out placing portions of UV-sterilized PRP-PCL scaffolds (1.33 cm^2) in 24-well plates to which 1 mL PBS was added and then incubated at 37 °C. At 4 hours, 1, 3 and 7 days samples (0.5 mL) of the release medium were collected, stored at −80 °C and replaced with fresh PBS. Total protein release was quantified by means of the BCA assay (Thermo Scientific Pierce; Rockford, IL, USA), using a BSA calibration line (0 to 2 mg/mL). PDBG-BB and VEGF were quantified using ELISA kits (RayBiotech; Norcross, GA, USA), according to the manufacturer’s instructions. Released TGF-β1 was quantified also with an ELISA kit after activation of the samples (100 μL) in 1N HCl (20 μL) for 10 min, followed by neutralization with 1.2 N NaOH/0.5 M HEPES (pH 7.2–7.6; 20 μL). In brief, samples of release medium were incubated in 96-well plates coated with monoclonal antibody to each growth factor for 2.5 h. The wells were washed, and biotinylated antibody was added and incubated for 1 h. After washing, HRP-conjugated streptavidin was added and wells were incubated for 45 min. Wells were washed, 3,3′,5,5′-tetramethylbenzidine substrate solution was added, and the wells were again incubated for 30 min, so color could develop in proportion to the amount of the corresponding growth factor. Finally, a stop solution was added to change the color from blue to yellow and absorbance was measured at 450 nm. A standard curve was used to determine the growth factor concentration.

2.3.5 Hemocompatibility—An activating complement test was carried out according to the UNE-ISO 10993-4 standard protocol. PCL scaffolds (1.33 cm^2) were incubated with

human plasma. After 15 minutes, complement activity was measured with the Complement Convertase assay (Haemoscan, Netherland).

2.3.6 Cytocompatibility—Cytocompatibility tests of PCL and PRP-PCL scaffolds were carried out in triplicate using murine fibroblasts (CCL-163, ATCC, USA) and human adipose-derived mesenchymal stem cells (MSC, Invitrogen, USA). Scaffold disks (1.33 cm^2) were sterilized in ethanol and placed in 24-well plates (LabClinics, Spain). Cells ($2{\cdot}10^4$ cells/well) were seeded in each well and cultured for 7 days in a humidified atmosphere with 5% CO_2 at 37 °C, renewing culture medium every second day. Fibroblasts were cultured in 1 mL DMEM medium (Dulbecco's modified Eagle's Medium F12-HAM, 10% fetal bovine serum, 13 μg/mL gentamicin), while MSC were cultured in 1 mL complete MesenPro medium (MesenPro RS, 10% growth supplement MesenPro RS, Gibco, USA) with antibiotics (penicillin 100 IU/mL and streptomycin 100 μg/mL). After incubation, cells were stained with calcein (1 mg/mL):propidium iodide (1 mg/mL):PBS (pH 7.4) 1:1:98 solution and again incubated in darkness for 10 minutes. Cell viability was evaluated from images obtained using a Laser Confocal Fluorescence Microscope (LCS, Leica Microsystems, Germany).

2.3.7 Cell attachment and proliferation—MSC proliferation on PCL and PRP-PCL scaffolds was evaluated using a MTT proliferation kit (Roche, Switzerland). Briefly, MSC ($2{\cdot}10^4$ cells/well) were cultured on the scaffolds in 24-well plates for up to 7 days in a humidified atmosphere with 5% CO_2 at 37°C. At the end of the culturing period, each sample was incubated for 4 hours with the MTT reagent at 37°C, and overnight with the detergent included in the kit. Final solutions were read at 550 nm (UV Bio-Rad Model 680 microplate reader, USA). The experiments were carried out in triplicate.

In parallel, cell attachment to the scaffolds was evaluated at 36 hours and 6 days. The culture medium was removed and the cells were fixed with paraformaldehyde (4%) for 10 minutes and washed with PBS 3 times. Then, 0.2 % (w/v) Triton in phosphate buffer pH 7.4 was added to the immobilized cells, which were then incubated for 5 minutes and washed three-times with PBS. The cell nuclei were stained with Hoescht dye solution (Sigma Aldrich, USA). After incubation for 30 minutes at dark, the fiber mats were washed again with phosphate buffer pH 7.4, mounted on glass slides using an anti-fading solution (Bio-Rad Laboratories, USA), and stored at −20°C for 24 h. The cells were visualized using a Confocal Spectral Microscope Leica TCS-SP2 (LEICA Microsystems Heidelberg GmbH, Mannheim, Germany). Counting of stained cell nuclei was performed, for two different pieces of scaffold, in 5 different fields of 0.25 mm^2.

Gene expression analysis of MSC was performed after cultured on PRP-PCL scaffolds using reverse transcriptase polymerase chain reaction (RT-PCR) and compared to that recorded for PCL scaffolds (non PRP-treated cells). The gene expression of collagen I and III and also lipoprotein lipase (LPL), osteocalcin (BGLAP), tenomodulin (TNMD) and aggrecan (ACAN) was recorded (n=3, for each group). Total RNA was extracted from 3, 7 and 14-day samples, purified using the Qiagen RNeasy Kit® and assessed for its purity and concentration of RNA by spectrophotometry. Quantitative real-time polymerase chain reaction was performed in triplicate as indicated by the manufacturer. TaqMan® gene

expression assay was used to analyze LPL, BGLAP, COL1A1, COL3A1, TNMD and ACAN expression (Hs 00173425_m1, Hs 01587814_g1, Hs 00164004_m1, Hs 00943809_m1, Hs00223332_m1, Hs 00153936_m1 respectively; Applied Biosystems, UK) and normalized against GAPDH (Hs 02758991_g1; Applied Biosystems, UK). Data were analyzed for relative expression using comparative cycle threshold (Ct) method. Results were referred to day 0 gene expression.

2.3.8 Angiogenic activity on chicken chorioallantoic membrane (CAM)—

Fertilized hen eggs were washed with 70% ethanol and incubated at 37°C and 60% RH. On day 3 albumen (2 mL) was aspirated from the acute pole of the egg to create a false air sac directly over the CAM, and a square window was cut with forceps. The window was closed with transparent tape and eggs were returned to incubation until day 8, when the sterilized PCL and PRP-PCL scaffolds were implanted. Then, incubation was continued until day 12 [25]. Finally, CAM was fixed with formaline 10% for 60 minutes, cut with a scalpel, transferred to a culture plate, cleaned with PBS and observed at 5×.

2.4 Statistical analysis

All results are reported as mean with associated standard deviation. Statistical analysis was performed using SPSS version 20, and a p value ≤ 0.05 was considered statistically significant. Furthermore, one-way ANOVA analysis with Tukey's LSD post-hoc test was used to evaluate differences between groups.

3. Results and Discussion

3.1 Preparation and characterization of PRP

PRP is attracting considerable attention for the bioactivation of scaffolds due to the simplicity, safety and cost-effectiveness of autologous blood preparation [26]. Freeze-thaw-freeze (FTF) cycles constitute an easy and inexpensive way to activate PRP retaining all proliferative and adhesive properties [22]. FTF enhances platelet lysis and cytokines expression avoiding the use of $CaCl_2$ or thrombin, which in turn interfere with cell proliferation and differentiation. Moreover, it has been previously proved that growth factors from frozen platelets remain viable after lyophilization [27]. In the freeze-dried activate PRP, contents in total protein and in VEGF were quantified as 79.5% (s.d. 1.4%) and 4.40 (s.d. 0.45) pg/mg, respectively.

Before PRP incorporation onto the PCL scaffold, several tests were carried out to confirm the ability of PRP to stimulate the proliferation of MSC. Cell growth was monitored for 11 days (Figure 1). Compared to the growth recorded in culture medium without PRP, addition of PRP (up to 10 vol.%; equivalent to 7.25 mg freeze-dried PRP/mL) remarkably enhanced the proliferation of MSC after 3 and 7 days, but differences decreased at day 11 because cells became confluent on the well surface. This finding is in agreement with previous reports on the positive effect of PRP at low concentration in culture medium, while high concentrations of PRP suppressed viability and proliferation [28]. Moreover, MSC cultured in the presence of 10 vol.% PRP produced more extracellular matrix (Alcian Blue staining of sulfated glycosaminoglycans, GAG). In contrast, typical staining of ALP (red points), an

early marker of osteoblast differentiation, was negative in both control and PRP-treated MSC, which indicates that the cells did not differentiate to osteoblast linage (Figure S1 in Supplementary Material). Although the literature about the effect of PRP on ALP activity is somehow contradictory, activation of ALP seems to depend on the presence of calcium during PRP activation or on the use of calcium-bearing scaffolds [29, 30]. The FTF method used in the present study to activate PRP prevented osteogenic differentiation of MSC. Moreover, the positive effect of PRP on MSC proliferation led to a higher extracellular matrix production as shown in the GAG concentration.

3.2 PCL electrospun fibers

PCL has suitable properties for electrospinning [14, 31]. 70–90 KDa PCL solution at 10 wt. % provided adequate viscosity for processing, resulting in fibers with intermediate degradation time. Solvents used in this study were DMF (high boiling point and polarity) and THF (low boiling point and polarity); both are Class 2 solvents (mid toxicity) in the European Pharmacopoeia, and THF is even considered Class 3 (low toxic potential) in The United States Pharmacopeia and The National Formulary (USP–NF). The mixture of both solvents was shown adequate to form homogeneous PCL solutions that were electrospinnable and afforded defect free nanofibers.

The fiber mats (0.8 mm thickness) were formed by nonwoven, porous interconnected structures with randomly dispersed nanofibers of diameter around 0.30–0.35 μm (Figure 2; greater magnifications in Figure S2 in Supplementary Material). Pore size ranged between 5 and 10 μm. This diameter could be easily tuned if required for a particular application [5]. Hydrolytic degradation of PCL scaffolds in phosphate buffer pH 7.4 resulted in loss of weight of ca. 10% after 50 days (Figure S3 in Supplementary Material), in agreement with previous reports [32]. Despite of having larger surface area, fiber mats of synthetic biodegradable polyesters degrade at slower rate than cast films because the acidic by-products of degradation at the ester bond, which autocatalyze the degradation reaction, can diffuse out of the scaffold structure more rapidly than from physically denser polymer films [33, 34]. Accelerated hydrolytic experiments carried out by immersion of the PCL fiber mats in NaOH 4M resulted in the disintegration of all specimens within a few minutes.

Preliminary screening of hemo- and cyto-compatibility of PCL scaffolds was carried out to ensure that no residual solvents or impurities might compromise their performance. PCL scaffold behaved as complement non-activating biomaterial (0.05 OD/24h/cm^2) [35] and showed an excellent compatibility with two cell lineages, murine fibroblasts and human MSC. Calcein-propidium iodide (live-dead) staining at day 7 showed a majority of viable cells with barely red (dead) staining, indicating good viability of both fibroblasts and MSC (Figure 3). In the case of fibroblasts, the roughness of the scaffold did not allow to capture all confocal planes, resulting in loss of information in the micrographs. Both cells types successfully attached and proliferated on PCL scaffolds after one week, confirming the suitability of the electrospun nanofibers as cell supports.

3.3 PRP-PCL scaffold

Once confirmed the bioactivity of PRP and the cytocompatibility of the PCL fibers, PRP-adsorbed PCL scaffolds were prepared. PCL scaffolds were sterilized prior PRP adsorption in order to avoid loss and inactivation of growth factors. Coating with PRP was carried out by impregnation followed by freeze-drying, as this latter technique has been previously shown not to alter the growth factors properties on proliferation and tissue regeneration [24, 27]. The density of the coating may depend on the concentration of growth factors and on the time that the scaffold remains immersed in PRP solution before freeze-drying. In our case, immersion of PCL in PRP solution (72.5 mg solids/mL) was carried for 4 hours at 4°C and resulted in 2.85 (s.d. 0.14) mg PRP per mg scaffold. The difference in weight among replicates was below 5%, which indicates quite uniform coating. FTIR analysis, SEM microphotographs and water contact angle values confirmed PRP adsorption on the scaffold structure.

No differences in the FTIR spectra of PCL were observed before and after electrospinning (Figure 4), which showed the characteristic assignments: CH_2 asymmetric and symmetric stretching at 2900–3000 and 2800–2900 cm^{-1}, respectively; C=O stretching at 1700–1760 cm^{-1}; CH scissoring and symmetric deformation at 1350–1480 cm^{-1}; O–C–O stretching at 1150–1200 cm^{-1}; C–O stretching at 1100–1150 cm^{-1}; C–C stretching at 1000–1100 cm^{-1}; C–O–C symmetric stretching at 900–1000 cm^{-1} and CH_2 rocking at 500–900 cm^{-1} [36]. The spectrum of freeze-dried PRP presented amide I and II peaks at 1660 and 1550 cm^{-1}, respectively, and a broad band in the 3300–3500 cm^{-1} region assigned to NH groups from proteins (3400–3500) and water (3300–3500) vibrations. Furthermore, PCL fibers coated with PRP exhibited a combination of bands found in both materials, being most significant the presence of the C=O stretching at 1700–1760 cm^{-1} from PCL, and the amide I and II at 1660 and 1550 cm^{-1} from proteins present in PRP. The peak at 2400 cm^{-1} in the spectrum of freeze-dried PRP can be attributed to CO_2 background, as the highly porous structure of the powder prevents tight compaction on the ATR crystal. PCL fibers coated with PRP did not present the CO_2 peak, indicating its removal from the scaffold.

In a preliminary test we observed that the freeze-drying process did not alter the nanofibrous structure of PCL scaffolds. Once processed with PRP, the appearance of the mat became different as PRP was homogeneously adsorbed on the scaffold in a sponge-like arrangement. Nevertheless, the average diameter of visible nanofibers was similar to that of pristine PCL fibers (Figure 2). Once immersed in culture medium, a PRP gel-like film was formed on the scaffold, supported by the solid nanofibers that provide the nanoscale architecture for cell attachment. Differently from the hydrophobic surface of PCL scaffold, which exhibited a mean water contact angle of 122° that remained constant for more than 5 minutes (Figure S4 in Supplementary Material), PRP coating led to highly hydrophilic surfaces. In fact, PRP-PCL scaffold absorbed the water drop in a few seconds, indicating that PRP has a hydrophilizing effect on the nanofibers. It has been previously demonstrated for collagen-immobilized PCL scaffolds that hydrophilization notably improves the attachment, spreading and proliferation of fibroblast cells compared to the pristine material [37]. Thus, the PRP-PCL scaffold containing growth factors and proteins could act as substrate for cell

attachment and create a microenvironment rich in growth factors that improves cell proliferation.

Since mechanical features are quite relevant for the success of the scaffold, the effects of the freeze-drying process and the coating with PRP were analyzed in detail. Freeze-drying of PCL solely scaffolds (without PRP) did not alter the Young's modulus, tensile stress and tensile strain (Figure 5). The Young's modulus values obtained for PCL fibers were in between those reported for PCL extruded films (190±6 MPa) and for other PCL porous electrospun mats (3.8±0.8 MPa) [38]. Further, the PRP coating did not significantly modify the Young's modulus compared to pristine nanofibers (54.50±15.09 vs. 42.32±15.09 MPa) and led to a minor decrease in tensile stress (7.46±0.84 vs. 10.78±3.01 MPa) and tensile strain (2.01±0.20 vs. 2.56±0.21 mm). These results suggest that the material becomes stiffer after PRP addition and can be torn apart more easily, although the small magnitude of these changes should not have negative repercussions on the potential clinical application of PCL electrospun fibers.

3.4 Growth factors release from PRP-PCL scaffolds

Since PRP has a complex composition, release experiments were carried out by monitoring the release of the total amount of protein and three representative growth factors from pieces (1.33 cm^2) of UV-sterilized PRP-PCL scaffolds immersed in PBS (Figure 6). A relevant amount of protein (9.63 mg) was released in the first 4 hours in PBS; at day 7, the amount of protein accumulated in the release medium was 11.18 mg (nearly 100% released). VEGF also showed a burst in the first hours of the test; the maximum amount released being 59.13 pg at day 7 (which corresponded to 94.3% initial loading). By contrast, TGF-β1 and PDGF-BB (the most potent isoform of PDGF) showed sustained release patterns. The amount of TGF-β1 in the medium progressively increased reaching a maximum at day 3, with ~684 pg released. PDGF-BB was released in a more sustained manner during the 7 days of the study; the amount released up to day 7 (1186 pg) was 2.6 times greater than that released during the first 4 h in PBS. This release behavior is in agreement with a recent report by Anitua and coworkers [39] on grade IV titanium discs coated with activated PRP, who found that PDGF was released in a more sustained way than VEGF or TGF-β1. Nevertheless, in our work the release was slightly slower, which is probably because PRP was more tightly embedded onto the PCL nanofibers, compared to the titanium surfaces. The greater retention can be favored by the fact that PRP was immobilized onto the PCL scaffold by means of freeze-drying, which may favor interactions with the substrate [40]. In this context, interactions between PDGF and alginate have been found responsible for the slower release of this growth factor, compared to the others, from alginate capsules [41]. It is interesting to note that the total amount released of each growth factor from the PRP-PCL scaffolds are slightly greater than those reported previously, which can be related to the fact that the PRP activation by means of freeze-thaw cycles as used in our study is more efficient in making the growth factors available from the platelets than activation using thrombin with $CaCl_2$ [22]. Moreover, the small dispersion of the values of the amount of growth factors released from several separately prepared PRP-coated scaffolds (Figure 6) is an index of the robustness of the preparation method.

3.5 MSC proliferation on PRP-PCL scaffolds

The effect of PRP on the attachment and proliferation of MSC on the scaffolds is summarized in Figure 7. MSC proliferation was found to be higher on PRP-PCL scaffold than on PCL scaffold; the differences becoming greater as the time progressed. PRP coating facilitated the wetting of the scaffold and made growth factors and cell recognition sites available to the cells, endowing the scaffold with high cell-loading properties. The progressive cell proliferation can be explained by the combined effect of the three growth factors monitored (see Figure 6). VEGF is known to stimulate MSC proliferation by activation and downstream signaling of PDGF receptors. Both PDGF-BB which is a potent mitogen, and TGF-β1 which increases MSC proliferation without bias towards the chondrogenic lineage [42], were sustainedly released from the scaffold, which led to higher proliferation levels as time progressed.

Cell viability on the PRP-PCL scaffold was evidenced by means of calcein-propidium iodide (live-dead) staining images of the MSC (Figure 8). After 7 days of incubation, PRP-PCL scaffolds were completely covered by cells, while pristine PCL fibers presented lower cell density. Although PCL fibers showed some autofluorescence, Hoechst staining enabled the quantification of MSC cells attached to the PRP-PCL and the PCL scaffolds after 36 h and 6 days (Figure S5 in Supplementary Material). MSC nuclei were stained in blue. According to the number of nuclei stained in blue, the number of MSC on PRP-PCL scaffolds was remarkably higher than on PCL scaffolds (Figure 9). After 36 h and 6 days, cell counting in the PRP-PCL scaffold was almost 2-fold and 5-fold greater than the cell count achieved with PCL scaffold. Thus, once again, the proliferating effect of PRP on MSC was evidenced.

RT-PCR analysis was performed to obtain additional data about the gene expression of various cell lineages and collagens markers (Figure 10). There was no expression of differentiation-related genes, which indicates that PRP did not induce MSC differentiation. After 3 days, the presence of PRP in the PCL scaffold decreased the expression of Col1a1, but this expression was induced at day 7 and then decreased at day 10. Col3a1 analysis did not result in any variation of gene expression between PCL scaffolds, regardless of the presence or absence of PRP. Expressions of differentiation factors were negative in all conditions, which suggests that there are no differentiation mechanisms in cells cultured with PRP and PCL-scaffold.

3.6 Angiogenic activity

CAM test has been proposed as an alternative method to animal experimentation to evaluate the biocompatibility of a material and, in particular, angiogenesis response [43, 44]. The growth of blood vessels in the chicken CAM during embryo development was analyzed after the contact of the CAM with PCL and PRP-PCL scaffolds for 5 days (Figure 11). Scaffold with PRP induced a notable angiogenic effect on the allantoic vessels density with a clear increase in the number of capillary blood vessels converging radially around the scaffold. PRP-PCL scaffolds were entrapped into the CAM, differently to the PCL scaffolds, which remained on the surface without appreciable interaction with CAM. Therefore, the gel rich in growth factors (VEGF, TGF-β1 and PDGF, among others) formed around the PRP-PCL

scaffold induced proliferation of epithelial and endothelial tissues, resulting in neovascularisation and CAM growth around the scaffold [24, 45].

Conclusion

The present study reports the development of an easy and effective procedure to treat PCL electrospun scaffolds with PRP for potential tissue engineering applications. Impregnation of PCL nanofibers by soaking in activated PRP followed by freeze-drying led to a solid support suitable for the handling of PRP without loss of activity. Coating with PRP notably improved hydrophilicity, mesenchymal stem cells attachment and proliferation on PCL scaffold, without inducing differentiation to a particular linage. Moreover PRP-PCL scaffolds were shown able to sustain the release of some growth factors, which may be useful for a sequential delivery of essential components for tissue regeneration. The results of this study prove the interest of PRP-PCL scaffolds as tissue engineering platforms by promoting cell attachment, proliferation and CAM angiogenesis. In vivo studies are needed to determine the recruitment effect of PRP-PCL scaffolds over the native cells.

Supplementary Material

Refer to Web version on PubMed Central for supplementary material.

Acknowledgments

Work supported by FEDER, Xunta de Galicia (10CSA203013PR), and MICINN (SAF2011-22771) Spain, and by NIH-NIGMS-NIA (grant # 1SC2AG036825-01) for which JM is gratefully acknowledged. L. Diaz-Gomez acknowledges MICINN for a FPI fellowship (BES-2012-051889). The authors thank Dr. A. Rey-Rico for the help in the initial steps of this work and P. Diaz-Rodriguez for support with VEGF quantification and valuable discussions.

References

1. Cooley, JF. GB Patent. 06385. 1900.
2. Formhals, A. US Patent. 1,975,504. 1934.
3. Sill TJ, von Recum A. Electrospinning: Applications in drug delivery and tissue engineering. Biomaterials. 1991; 29:1989–2006. [PubMed: 18281090]
4. Deitzel JM, Kleinmeyer J, Harris DC, Beck NC. The effect of variables on the morphology of electrospun nanofibers and textiles. Polymer. 2001; 42:261–272.
5. Cui W, Zhou Y, Chang J. Electrospun nanofibrous materials for tissue engineering and drug delivery. Sci Technol Adv Mat. 2010; 11:014108.
6. Jang JH, Castano O, Kim HW. Electrospun materials as potential platforms for bone tissue engineering. Adv Drug Deliv Rev. 2009; 61:1065–1083. [PubMed: 19646493]
7. Moffat KL, Kwei ASP, Spalazzi JP, Doty SB, Levine WN, Lu HH. Novel nanofiber-based scaffold for rotator cuff repair and augmentation. Tissue Eng. 2009; 15:115–126.
8. Xie J, Li X, Lipner J, Manning CN, Schwartz AG, Thomopoulos S, Xia Y. “Aligned-to-random” nanofiber scaffolds for mimicking the structure of the tendon-to-bone insertion site. Nanoscale. 2010; 2:923–926. [PubMed: 20648290]
9. Zhang X, Thomas V, Xu Y, Bellis SL, Vohra YK. An in vitro regenerated functional human endothelium on a nanofibrous electrospun scaffold. Biomaterials. 2010; 31:4376–4381. [PubMed: 20199808]
10. Venugopal J, Ramakrishna S. Applications of polymer nanofibers in biomedicine and biotechnology. Appl Biochem Biotech. 2005; 125:147–157.

11. Prabhakaran MP, Venugopal J, Ramakrishna S. Electrospun nanostructured scaffolds for bone tissue engineering. Acta Biomaterialia. 2009; 5:2884–2893. [PubMed: 19447211]
12. Ji W, Sun Y, Yang F, vanden Beucken JJJP, Fan M, Chen Z, Jansen JA. Bioactive electrospun scaffolds delivering growth factors and genes for tissue engineering applications. Pharm Res. 2011; 28:1259–1272. [PubMed: 21088985]
13. Luong-Van E, Grondahl L, Chua KN, Leong KW, Nurcombe V, Cool SM. Controlled release of heparin from poly(ε-caprolactone) electrospun fibers. Biomaterials. 2006; 27:2042–2050. [PubMed: 16305806]
14. Sarasam A, Madihally SV. Characterization of chitosan–polycaprolactone blends for tissue engineering applications. Biomaterials. 2005; 26:5500–5508. [PubMed: 15860206]
15. Yoo HS, Kim TG, Park TG. Surface-functionalized electrospun nanofibers for tissue engineering and drug delivery. Adv Drug Deliver Rev. 2009; 61:1033–1042.
16. Lee J, Yoo JJ, Atala A, Lee SJ. The effect of controlled release of PDGF-BB from heparin-conjugated electrospun PCL/gelatin scaffolds on cellular bioactivity and infiltration. Biomaterials. 2012; 33:6709–6720. [PubMed: 22770570]
17. Casper CL, Yamaguchi N, Kiick KL, Rabolt JF. Functionalizing electrospun fibers with biologically relevant macromolecules. Biomacromolecules. 2005; 6:1998–2007. [PubMed: 16004438]
18. Yao C, Li X, Neohb KG, Shib Z, Kang ET. Surface modification and antibacterial activity of electrospun polyurethane fibrous membranes with quaternary ammonium moieties. J Membrane Sci. 2008; 320:259–267.
19. Marx RE. Platelet-rich plasma: evidence to support its use. J Oral Maxil Surg. 2004; 64:489–496.
20. Reed GL. Platelet secretory mechanisms. Semin Thromb Hemos. 2004; 30:441–450.
21. Tayalia P, Mooney DJ. Controlled growth factor delivery for tissue engineering. Adv Mater. 2009; 21:3269–3285. [PubMed: 20882497]
22. Sell SA, Wolfe PS, Ericksen JJ, Simpson DG, Bowlin GL. Incorporating platelet-rich plasma into electrospun scaffolds for tissue engineering applications. Tissue Eng. 2001; 17:2723–2737.
23. Kutlu B, Aydın RST, Akman AC, Gümüşderelioglu M, Nohutcu RM. Platelet-rich plasma-loaded chitosan scaffolds: Preparation and growth factor release kinetics. J Biomed Mater Res B Appl Biomater. 2013; 101:28–35. [PubMed: 22987323]
24. Nakajima Y, Kawase T, Kobayashi M, Okuda K, Wolff LF, Yoshie H. Bioactivity of freeze-dried platelet-rich plasma in an adsorbed form on a biodegradable polymer material. Platelets. 2012; 23:594–603. [PubMed: 22273512]
25. Ribatti D, Nico B, Vacca A, Presta M. The gelatin sponge–chorioallantoic membrane assay. Nature protocols. 2006; 1:85–91.
26. Anitua E, Sanchez M, Orive G, Andia I. The potential impact of the preparation rich in growth factors (PRGF) in different medical fields. Biomaterials. 2007; 28:4551–4560. [PubMed: 17659771]
27. Pietramaggiori G, Kaipainen A, Czeczuga JM, Wagner CT, Orgill DP. Freeze-dried plalelet-rich plasma shows beneficial healing properties in chronic wounds. Wound Repair Regen. 2006; 14:573–80. [PubMed: 17014669]
28. Choi BH, Zhu SJ, Kim BY, Huh JY, Lee SH, Jung JH. Effect of platelet-rich plasma (PRP) concentration on the viability and proliferation of alveolar bone cells: an in vitro study. Int J Oral Maxillofac Surg. 2005; 34:420–424. [PubMed: 16053853]
29. Kilian O, Alt V, Heiss C, Jonuleit T, Dingeldein E, Flesch I, Fidorra U, Wenisch S, Schnettler R. New blood vessel formation and expression of VEGF receptors after implantation of platelet growth factor-enriched biodegradable nanocrystalline hydroxyapatite. Growth Factors. 2005; 23:125–133. [PubMed: 16019434]
30. Kasten P, Vogel J, Beyen I, Weiss S, Niemeyer P, Leo A, Lüginbuhl R. Effect of platelet-rich plasma on the in vitro proliferation and osteogenic differentiation of human mesenchymal stem cells on distinct calcium phosphate scaffolds: the specific surface area makes a difference. J Biomater Appl. 2008; 23:169–188. [PubMed: 18632770]

31. Yoshimoto H, Shin YM, Terai H, Vacanti JP. A biodegradable nanofiber scaffold by electrospinning and its potential for bone tissue engineering. Biomaterials. 2003; 24:2077–2082. [PubMed: 12628828]
32. Bölgen N, Menceloğlu YZ, Acatay K, Vargel I, Pişkin E. In vitro and in vivo degradation of non-woven materials made of poly(epsilon-caprolactone) nanofibers prepared by electrospinning under different conditions. J Biomater Sci Polym Ed. 2005; 16:1537–55. [PubMed: 16366336]
33. Kim K, Yua M, Zonga X, Chiuc J, Fangb D, Seod YS, Hsiao BS, Chu B, Hadjiargyrou M. Control of degradation rate and hydrophilicity in electrospun non-woven poly(d,l-lactide) nanofiber scaffolds for biomedical applications. Biomaterials. 2003; 24:4977–4985. [PubMed: 14559011]
34. Cipitria A, Skelton A, Dargaville TR, Dalton PD, Hutmacher DW. Design, fabrication and characterization of PCL electrospun scaffolds a review. J Mater Chem. 2011; 21:9419–9453.
35. Meek MF, Jansen K, Steendam R, van Oeveren W, van Wachem PB, van Luyn MJA. J Biomed Mater Res A. 2003; 68:43–51. [PubMed: 14661248]
36. Qin X, Wu D. Effect of different solvents on poly(caprolactone) (PCL) electrospun nonwoven membranes. J Therm Anal Calorim. 2012; 107:1007–1013.
37. Duan Y, Wang Z, Yan W, Wang S, Zhang S, Jia J. Preparation of collagen-coated electrospun nanofibers by remote plasma treatment and their biological properties. J Biomater Sci Polym Ed. 2007; 18:1153–1164. [PubMed: 17931505]
38. Croisier F, Duwez AS, Jérôme C, Léonard AF, van der Werf KO, Dijkstra PJ, Bennink ML. Mechanical testing of electrospun PCL fibers. Acta Biomater. 2012; 8:218–224. [PubMed: 21878398]
39. Sanchez-Ilarduya MB, Trouche E, Tejero R, Orive G, Reviakine I, Anitua E. Time-dependent release of growth factors from implant surfaces treated with plasma rich in growth factors. J Biomed Mater Res Part A. 2013; 101:1478–1488.
40. Kutlu B, Aydin RST, Akman AC, Gümüsderelioglu M, Nohutcu RM. Platelet-rich plasma-loaded chitosan scaffolds: preparation and growth factor release kinetics. J Biomed Mater Res Part B: Appl Biomater. 2013; 101:28–35. [PubMed: 22987323]
41. Lu HH, Vo JM, Chin HS, Lin J, Cozin M, Tsay R, Eisig S, Landesberg R. Controlled delivery of platelet-rich plasma-derived growth factors for bone formation. J Biomed Mater Res. 2008; 86A: 1128–1136.
42. Rodrigues M, Griffith LG, Wells A. Growth factor regulation of proliferation and survival of multipotential stromal cells. Stem Cell Res Ther. 2010; 1:32. [PubMed: 20977782]
43. Valdes TI, Kreutzer D, Moussy F. The chick chorioallantoic membrane as a novel in vivo model for the testing of biomaterials. J Biomed Mater Res. 2002; 62:273–282. [PubMed: 12209948]
44. Cazedey ECL, Carvalho FC, Fiorentino FAM, Gremião MPD, Salgado HRN. Corrositex®, BCOP and HET-CAM as alternative methods to animal experimentation. Braz J Pharm Sci. 2009; 45:759–766.
45. Singh S, Wu BM, Dunn JCY. Delivery of VEGF using collagen-coated polycaprolactone scaffolds stimulates angiogenesis. J Biomed Mater Res A. 2012; 100:720–727. [PubMed: 22213643]

Highlights

- Platelet-rich plasma (PRP) can be adsorbed on electrospun fibers via lyophilization
- PRP coating enhanced mesenchymal stem cells adhesion and proliferation on scaffolds
- PRP-coated scaffolds showed sustained release of growth factors
- Adsorbed PRP provided angiogenic features
- PRP-poly(ε-caprolactone) scaffolds hold promise for tissue regeneration applications

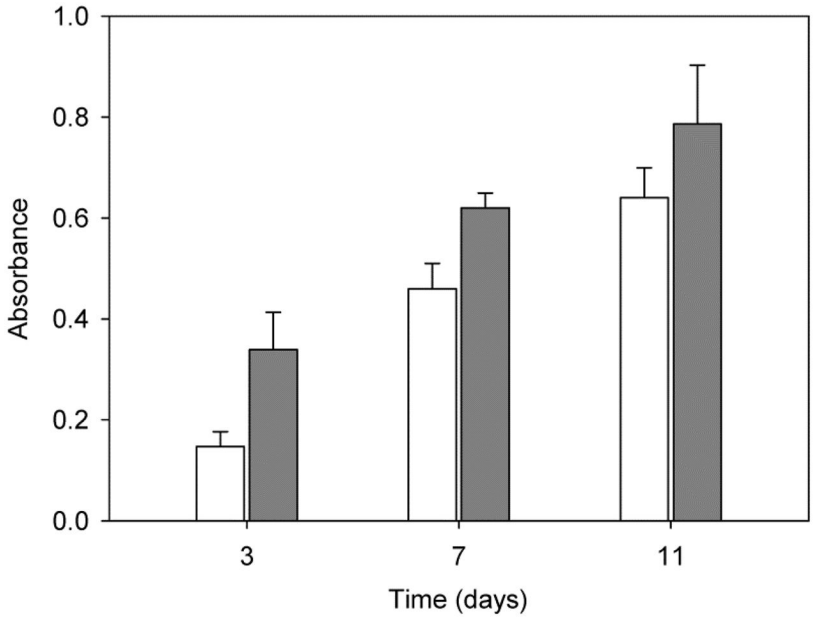

Figure 1.

Effect of addition of PRP into culture medium on the proliferation of human MSC. Cells ($2{\cdot}10^4$) were seeded in 1 mL of MSC medium (control; white columns) or in 1 mL of PRP-rich medium (grey columns) and proliferation (MTT) was measured at 3, 7 and 11 days. Error bars represent standard deviations of three independent experiments.

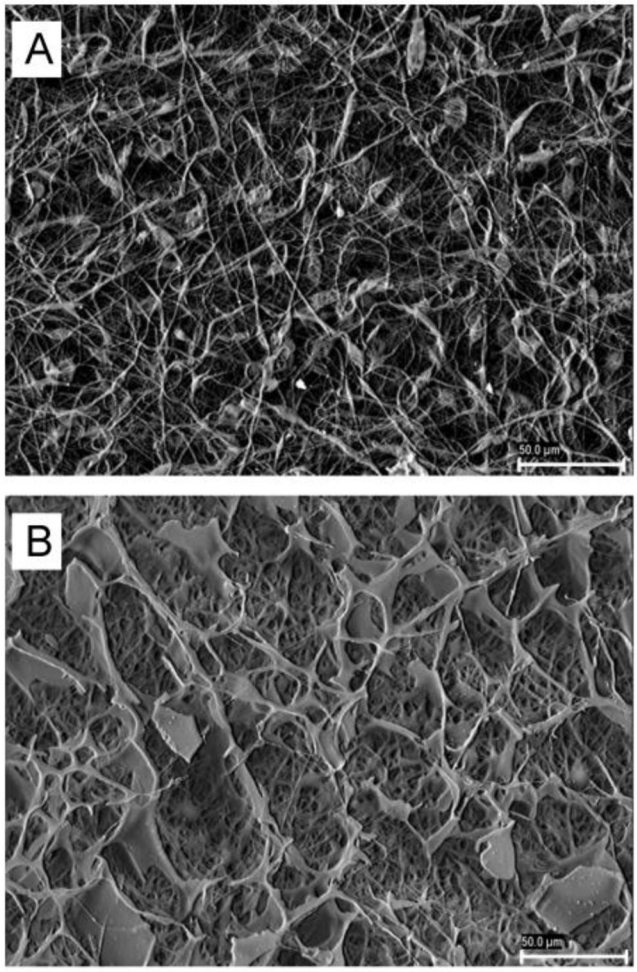

Figure 2.
SEM microphotographs of pristine PCL (A) and PRP-PCL (B) scaffolds at 1000×. Scale bar is 50 μm.

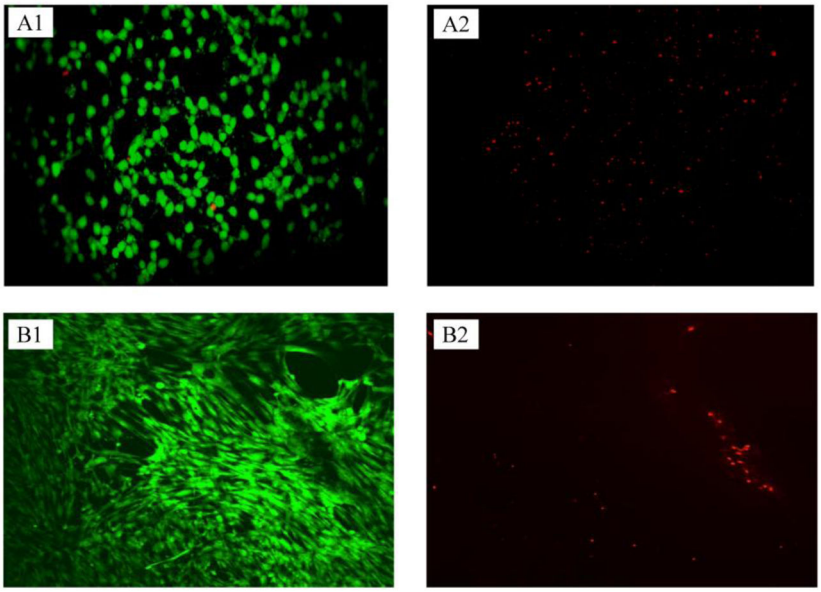

Figure 3.

Calcein (left)-propidium iodide (right) staining of fibroblasts (A) and MSC (B) grown on PCL scaffolds after 7 days. The green stains on left column show live cells and red stains on the right column show dead cells.

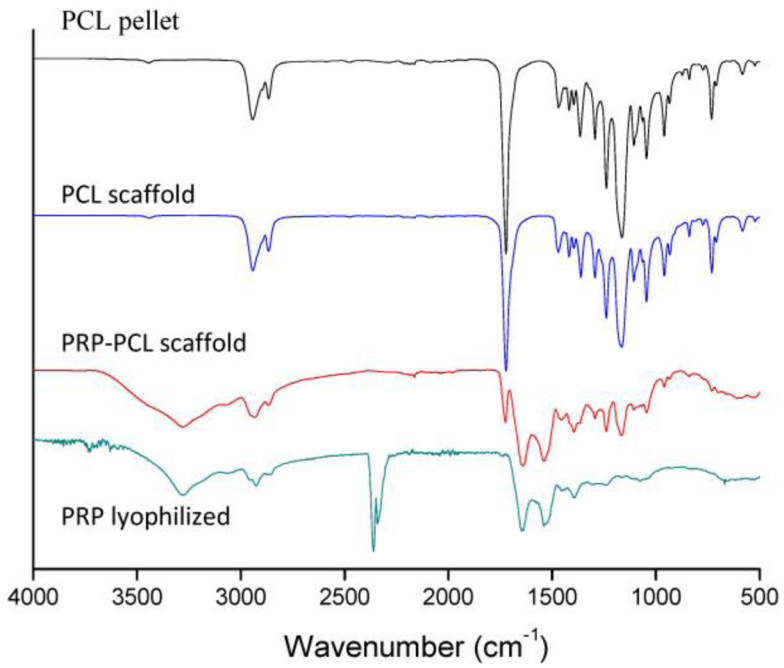

Figure 4.

FTIR spectra of lyophilized PRP, PCL pellet, and PCL and PRP-PCL scaffolds. PRP-PCL scaffolds exhibited a combination of bands found in both PRP (mainly amide I and II at 1660 and 1550 cm^{-1}) and PCL (C=O stretching at 1700–1760 cm^{-1}). The peak at 2400 cm^{-1} in the spectrum of lyophilized PRP was due to CO_2 background.

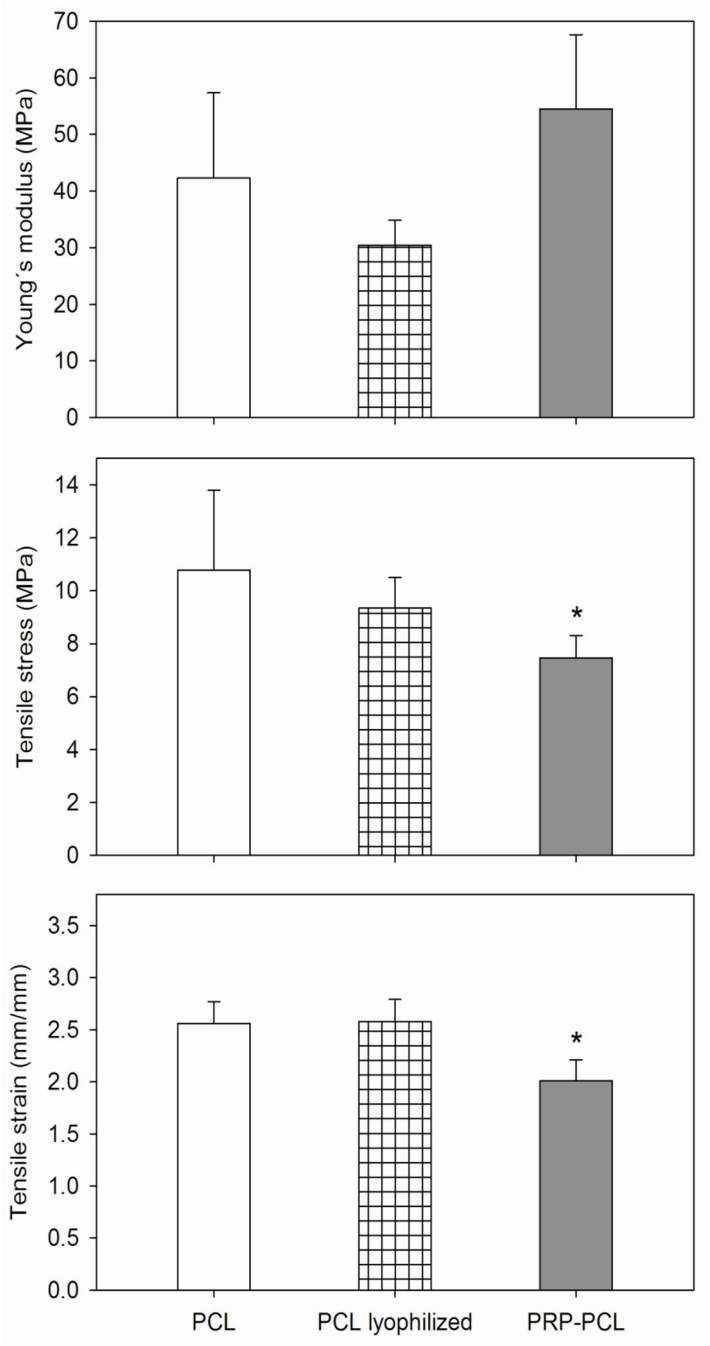

Figure 5.

Young's modulus, tensile stress and tensile strain of pristine PCL scaffolds (white columns), freeze-dried PCL solely scaffolds (striped columns), and PRP-PCL scaffolds (grey columns). Statistically significant differences ($p > 0.05$) of the PCL nanofibers upon adsorption of PRP compared to pristine PCL nanofibers are indicated with an asterisk.

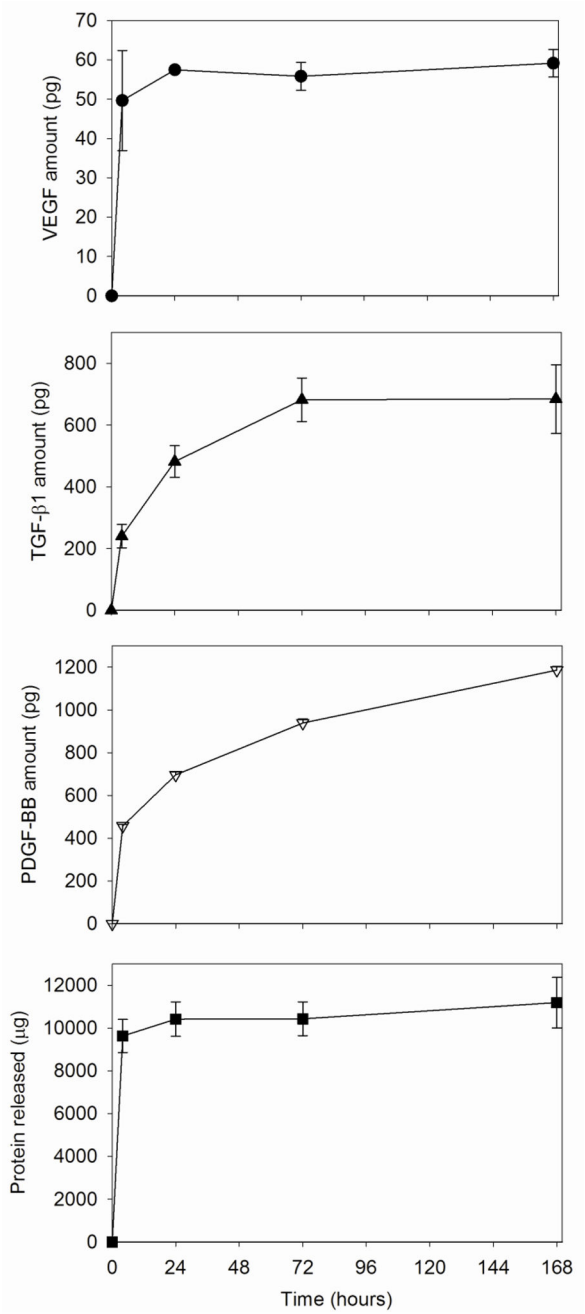

Figure 6.

Cumulative release profiles of total protein and of growth factors PDGF-BB, TGF-β1, and VEGF from UV-sterilized PRP-PCL scaffolds (1.33 cm^2) in PBS at 37°C.

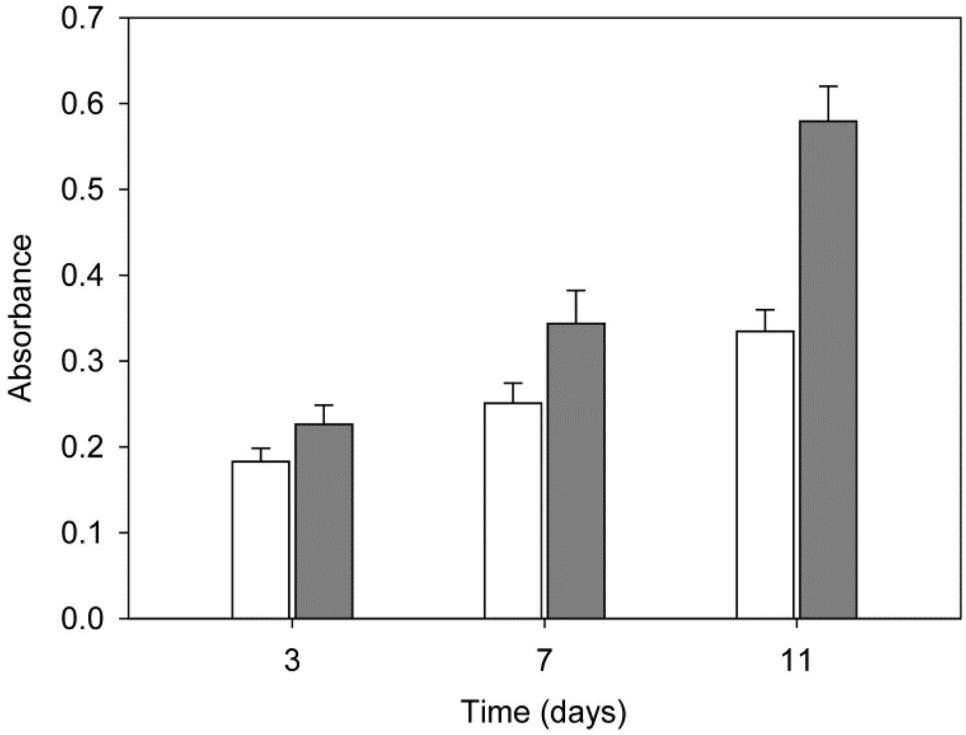

Figure 7.
MSC proliferation on the PCL (white columns) and PRP-PCL (grey columns) scaffolds at 1, 3 and 7 days.

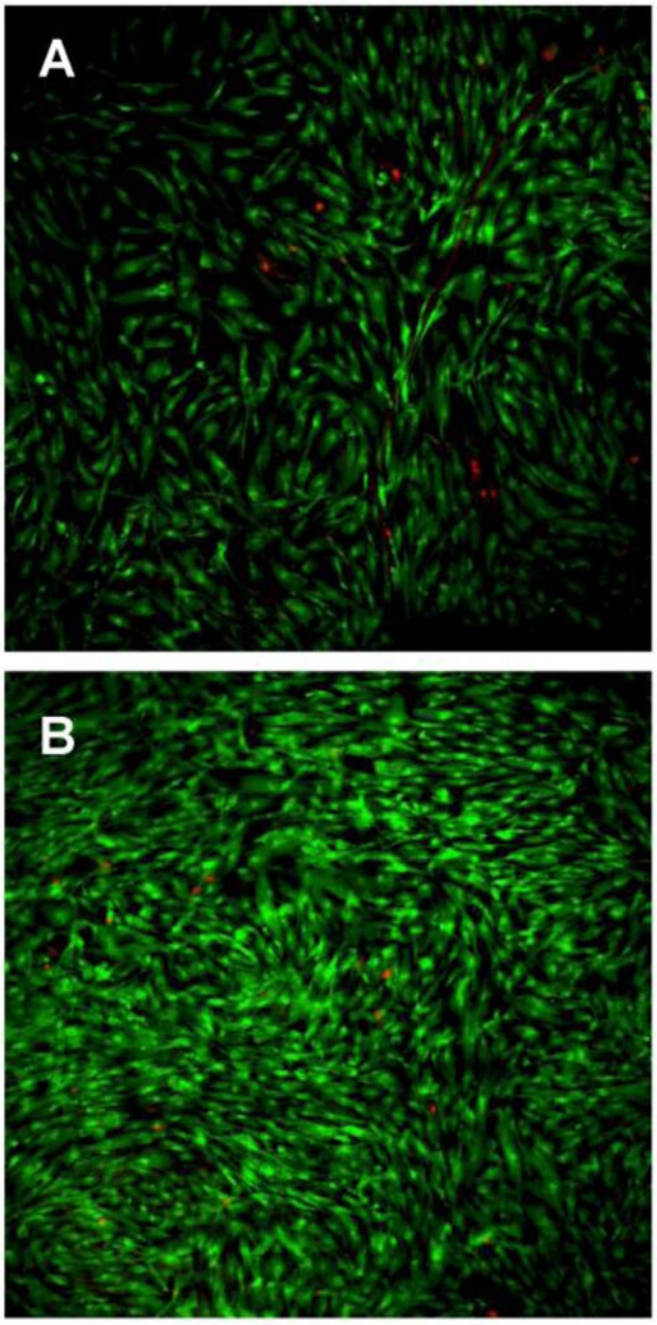

Figure 8.
Live-dead staining images of MSC grown on PCL (A) and PRP-PCL (B) scaffolds after 6 days incubation. Live cells are shown in green and dead cells in red.

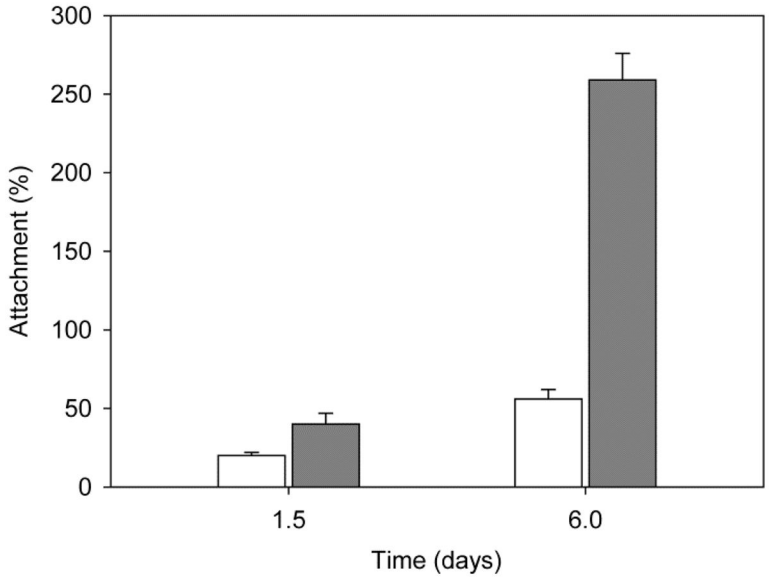

Figure 9.

Number of cells attached to PCL (white column) and PRP-PCL (grey column) scaffolds expressed as percentage of the seeding density after 1.5 and 6 days.

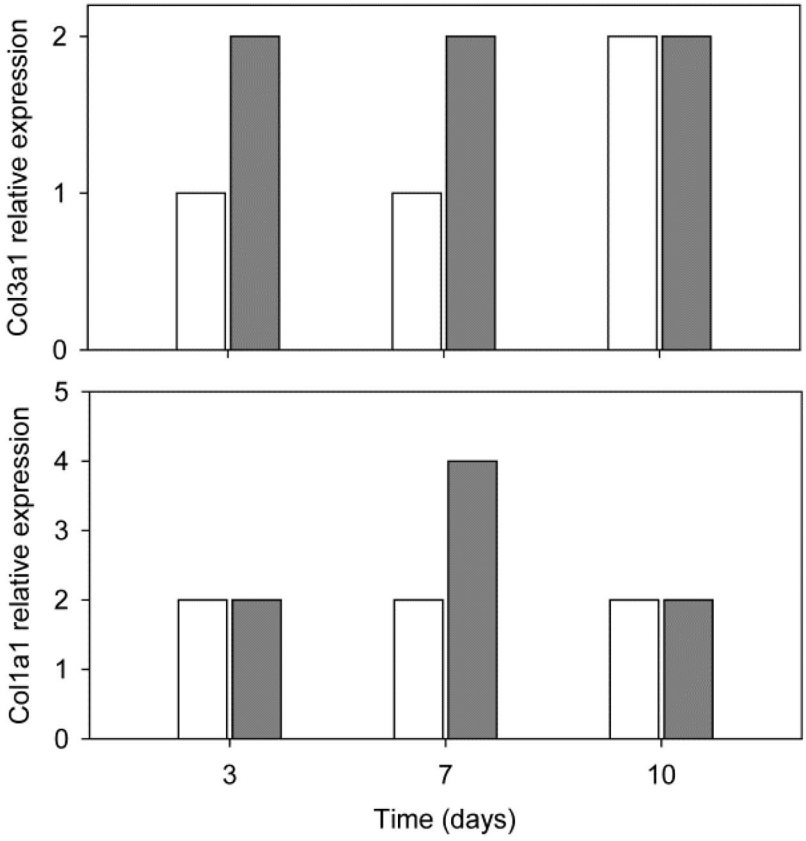

Figure 10.

Reverse transcriptase polymerase chain reaction (RT-PCR) measured expression of Col1a1 and Col3a1 in MSC grown on PCL (white columns) and PRP-PCL (grey columns) scaffolds at 3, 7 and 10 days.

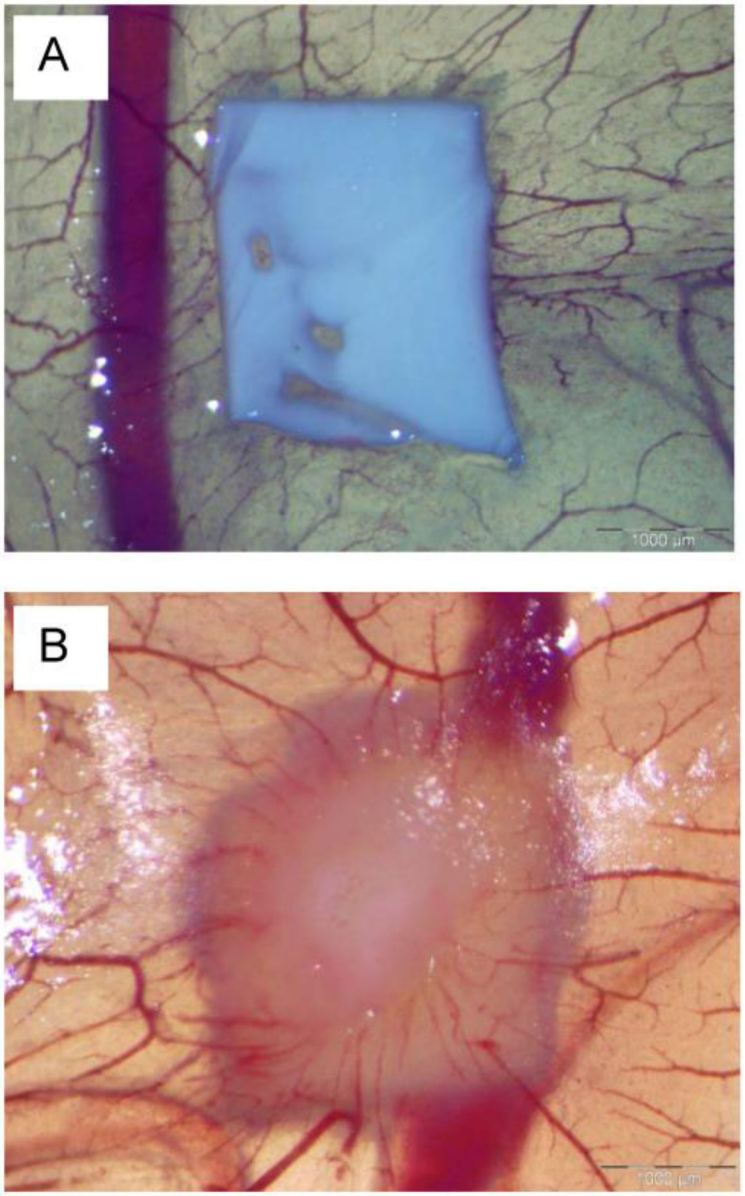

Figure 11.
Effect of PCL (A) and PRP-PCL (B) scaffolds on CAM angiogenesis at day 12 of incubation of fertilized hen eggs.